

Evidence of drugs confinement into silica mesoporous matrices by STEM Cs corrected microscopy

María Vallet-Regí,^{*a,b} Miguel Manzano,^{a,b} José M. González-Calbet^{*c} and Eiji Okunishi^d

^a Departamento de Química Inorgánica y Bioinorgánica. Facultad de Farmacia. Universidad Complutense de Madrid. 28040 Spain. Fax: +34 913941786; Tel: +34 913941843; E-mail: vallet@farm.ucm.es

^b Centro de Investigación Biomédica en Red. Bioingeniería, Biomateriales y Nanomedicina, CIBER-BBN, Spain.

^c Departamento de Química Inorgánica I. Facultad de Ciencias Químicas. Universidad Complutense de Madrid. 28040 Spain. Fax: +34 913944352; Tel: +34 913944342; E-mail: jgcalbet@quim.ucm.es

^d JEOL Ltd., 196-8558 Japan. Fax: +81 425468063; Tel: +81 425422152; E-mail: okunishi@jeol.co.jp

Supporting Information

S1. Materials and Methods

SBA 15 ordered mesoporous materials were produced according to the literature.¹ The template solution was prepared dissolving 4g of Pluronic[®] P123 (kindly supplied by BASF Corporation) in 138 mL of deionized water and 10.3 mL of HCl (37 wt%, Aldrich) under magnetic stirring. When the surfactant was completely dissolved, 8.2 mL of tetraethyl orthosilicate (TEOS, Aldrich) were added to the template solution to yield a molar composition of 1.0 Si(OEt)₄ : 0.017 P123 : 3.4 HCl : 208.3 H₂O. The resulting mixture was kept under magnetic stirring for 12 h at 308 K in a sealed Teflon container and subsequently aged at 373 K for 24 h. Solid silica particles were then filtered, washed with deionized water and dried at 333 K for 12h. The surfactant was removed by thermal treatment, which was carried out at 823 K under N₂ flow for 2h and then under atmospheric air for further 2 h. Surfactant removal was confirmed by thermal techniques.

Chemical modification of the silica mesopore walls was carried out by reacting 500 mg of template-free mesoporous materials with 2.5 mmol of 3-aminopropyl triethoxysilane (APTES: ABCR GmbH, Germany) in toluene (Aldrich). The whole reacting system together with the mesoporous material was purged with Ar gas for 2 h before the addition of APTES, so inert atmosphere was achieved within the system. Reactions were performed under reflux conditions for 16 hours and the products were

filtered and washed with a mixture of toluene and diethyl ether (1:1). Amine-functionalised mesoporous silica materials were dried at 333K for 12 h in air.

S2. Instrumentation

X-ray diffraction: Ordered mesoporous materials were analysed using powder X-ray diffraction at small angles (SA-XRD) in a Philips X'Pert diffractometer (Philips electronics NV, Eindhoven, Netherlands) with Bragg-Brentano geometry.

X-ray fluorescence: The total amount of phosphorus was determined by X-ray fluorescence (XRF) using a Philips PANalytical AXIOS spectrometer (Philips Electronics NV). X-ray were generated using the RhK_α line at $\lambda = 0.614 \text{ \AA}$. The composition of samples was measured by balancing the oxygen content in every specimen.

Nitrogen adsorption: The surface characterisation of materials was carried out by N_2 adsorption/desorption analysis at 77 K on a Micromeritics ASAP2020 analyzer (Micromeritics Co, Norcross GA, USA). In all cases, 50-70 mg of material was degassed at 423 K for 24 h under a vacuum lower than 10^{-5} torr before the analysis.

Scanning Transmission Electronic Microscopy: STEM was carried out using a JEM-ARM200F electron microscope equipped with a STEM Cs corrector able to perform analysis with a resolution of 0.08 nm and with an accessory of electron energy loss spectrometer (Gatan Enfina) located at the demonstration room of JEOL Ltd. At Akishima Tokyo, Japan.

FTIR Spectroscopy: Fourier Transformed Infra Red (FTIR) spectra of mesoporous materials were collected in a Thermo Nicolet Nexus equipped with a Goldengate attenuated total reflectance (ATR) device. FTIR spectra were smoothed and wavenumbers of the bands were determined using the Omnic spectroscopic software from Thermo Nicolet Corporation.

S3. Characterisation

SBA 15 isotherms can be clearly attributed to a type IV in the BDDT classification,² with the typical hysteresis loops of this type of mesoporous materials. (Figure S1). The parallel adsorption and desorption branches confirm the cylindrical

mesopores with narrow pore size distribution. Three different regions can be observed on the isotherm plots: (1) a linear region due to multilayer adsorption in mesopores; (2) a steep region due to capillary condensation within these mesopores; (3) a last linear region due to multilayer formation onto the external surface of the grains. It is worthy to mention that after both processes of drug loading and surface functionalisation, the mesostructured arrangement of the matrices survived both processes, since the hysteresis loops present similar shape.

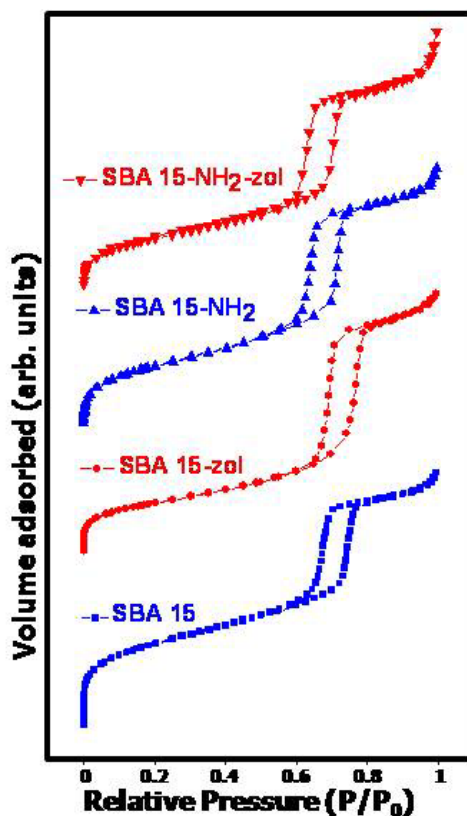


Figure S1. N₂ adsorption isotherms of SBA 15, SBA 15 loaded with zoledronate, SBA 15-NH₂ and SBA 15-NH₂ loaded with zoledronate.

The small angle XRD patterns of SBA 15 (Figure S2) showed three clear maxima at 0.9°, 1.6° and 1.8° 2 θ . These reflections can be assigned to [100], [110], and [200] directions of a hexagonal planar symmetry (*p6mm*). When SBA 15 was loaded with zoledronate and functionalised with amine groups, the obtained XRD patterns showed small differences from the conventional material, but the same diffraction maxima. This suggests the same hexagonal symmetry of the mesopores, which confirm the prevalence of the ordered mesostructure after both processes.

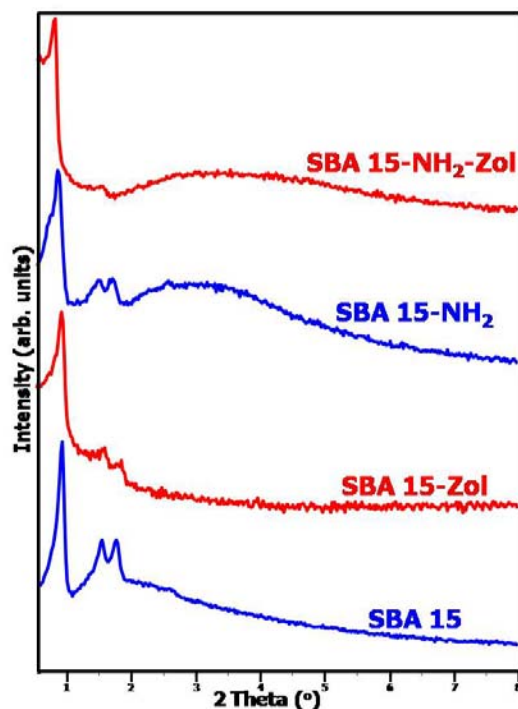


Figure S2. XRD patterns of SBA 15, SBA 15 loaded with zoledronate, SBA 15-NH₂ and SBA 15-NH₂ loaded with zoledronate.

FTIR spectra of SBA 15 matrix (Figure S3) showed the characteristic vibration bands of this type of silica materials, that is, asymmetric stretching Si-O-Si (ν_{SiOSi}) at *ca.* 1085 cm^{-1} , symmetric stretching Si-O (ν_{SiO}) at *ca.* 800 cm^{-1} , Si-O-Si bending (δ_{SiOSi}) at *ca.* 470 cm^{-1} and stretching vibrations of Si-OH (ν_{SiOH}) groups at *ca.* 960 cm^{-1} . A broad band with a maximum near 3400 cm^{-1} is attributed to the O-H stretching band corresponding to both Si-OH groups and some physisorbed water (the latter was confirmed by the presence of HOH deformation band at *ca.* 1620 cm^{-1}).

After loading the SBA 15 matrix with zoledronate, the most characteristic vibration bands from bisphosphonates, stretching P=O (1200-1160 cm^{-1}), stretching P-OH (≈ 1000 and ≈ 925 cm^{-1}) and deformation POH (*ca.* 1080 cm^{-1}), were overlapped by SBA 15 vibration bands. However, it is possible to observe a small shoulder in the broad O-H stretching band at *ca.* 2900 and 2800 cm^{-1} , which unequivocally represents the presence of C-H bonds (anti-symmetric and symmetric C-H stretching bands), and, consequently, confirms the presence of the alkyl chain from the drug. Additionally, the presence of zoledronate ([1-Hydroxy-2-(1H-imidazol-1-yl)-ethylidene]bisphosphonic acid) can be assured by the presence of the imidazole ring skeleton vibrations at *ca.*

1500 cm^{-1} and the asymmetric and symmetric ring $\text{C}=\text{C}$ stretching vibrations at *ca.* 1450 cm^{-1} .

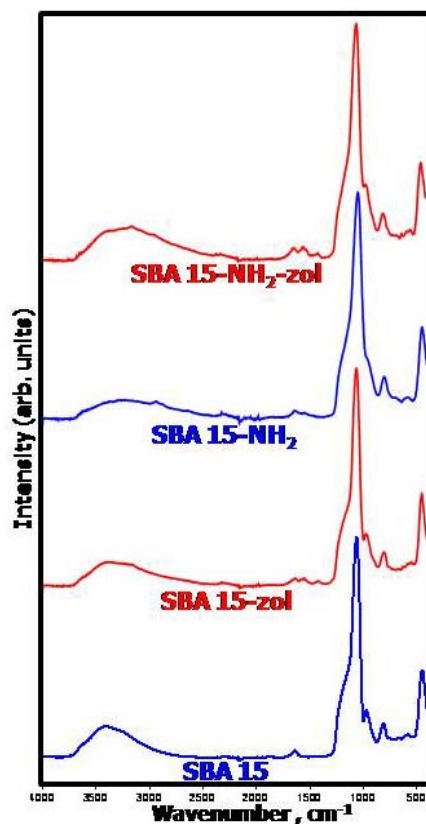


Figure S3. FTIR spectra of SBA 15, SBA 15 loaded with zoledronate, SBA 15-NH₂ and SBA 15-NH₂ loaded with zoledronate.

The success of the amine modification was confirmed by the presence of typical amine group stretching vibration bands (ν_{NH}) at *ca.* 3500 cm^{-1} . The presence of amine groups was also confirmed with the δ_{NH} bands at *ca.* 1500 cm^{-1} . The presence of absorption bands at *ca.* 2900 and 2800 cm^{-1} are attributed to C-H stretching vibrations (ν_{CH}) from the PrNH₂ groups. When loading these functionalised matrices with zoledronate, the only vibration band that was not overlapped was the ring $\text{C}=\text{C}$ stretching vibrations at *ca.* 1450 cm^{-1} , which can be observed in Figure S3 (SBA 15-NH₂-zol) and confirms the drug loading into the amine functionalised matrix.

References

¹ D.Y. Zhao, Q.S. Huo, J.L. Feng, B.F. Chmelka, G.D. Stucky. *J. Am. Chem. Soc.*, 1998, **120**, 6024.

² S.J. Gregg, K.S.W. Sing, Academic Press, London, 1982, 2nd ed.